

Discrete diffraction in an optically induced lattice in photorefractive media with a quadratic electro-optic effect

G. STAROŃ, E. WEINERT-RĄCZKA*, and P. URBAN

Department of Electrical Engineering, Szczecin University of Technology,
17 Piastów Ave., 70–310 Szczecin, Poland

Propagation of light in an optically induced waveguide array in biased photorefractive media with a quadratic electro-optic effect is investigated numerically with the beam propagation method. The refractive index distribution of the array is induced by two coherent plane waves interfering in a guiding layer in a photorefractive multiple quantum well (MQW) planar waveguide. The influence of modulation depth and the space period of an interference pattern as well as the external electric field intensity on diffraction properties of the array is analysed. The potential possibility of all-optical switching due to the dependence of the guided wave output distribution on the external waves parameters is shown.

Keywords: discrete diffraction, optically induced lattice, photorefractive effect.

1. Introduction

Propagation of light in arrays of waveguides has been the subject of intensive research for years (see Ref. 1 for review). Light in the array is guided by individual channels so narrow beams do not experience widening caused by traditional diffraction. Spreading of the beam occurs due to the coupling between adjacent waveguides. The properties of such a discrete diffraction are different from diffraction in uniform media. The output distribution of power depends on the coupling coefficient. The diffraction can be managed from normal to zero and anomalous depending on the beam incidence angle [2]. The influence of light intensity on the refractive index distribution appearing in nonlinear materials makes it possible to control optically discrete diffraction strength, which leads to the propagation of self-trapped beams called discrete solitons. In review works [1,3,4], the potential applications of this phenomenon in all-optical signal steering are emphasized. In the last few years, a lot of works dedicated to propagation of narrow beams in optically induced waveguide systems have appeared [5–10]. The systems of this type allow to control array parameters during the experiment, which can be used in switching. A lot of interesting issues are connected with the nonlinear interaction between guided wave and optically induced periodic structure (the lattice) [11,12]. Optically induced lattices (OIL) divide into two groups. In one of them waveguide arrays are induced by interfering plane waves and have sine-shape refractive index distribution with the space period and amplitude dependent on the writing beams parameters [5–11]. In the other group, periodic

structures are created by sets of parallel beams [12,13]. In such a case, refractive index distribution depends on the transverse shape of the beams and the distance between them. Lattices are usually induced in materials with the strong nonlinear response, such as photorefractive crystals, e.g., SBN [6–9]. So far, we have not met works dedicated to propagation in a lattice induced in photorefractive material with quadratic electrooptic effect, where the possibility of obtaining high refractive index changes is an advantage.

In this work we analyse light propagation in one dimensional waveguide array optically induced in biased photorefractive material with quadratic relationship between refractive index and electric field. As an example, we consider a multiple quantum wells (MQW) planar waveguide [14] with the lattice induced by two interfering plane waves. The advantage of this system is the possibility of regulation not only the period and amplitude but also the shape of induced waveguides by changing the external electric field or the interference pattern modulation depth. As a result, the continuous regulation of coupling between induced waveguides can be obtained. Additionally, if the structure has the geometry of a planar waveguide and waves, which generate the lattice, propagate across the thin guiding layer, the system makes it possible to use the external waves with resonant frequencies. The high absorption in this spectral range allows us to use very small light intensities without a significant increase in switching time.

2. Formulation of the problem

Two plane waves interfering within the guiding layer of a photorefractive waveguide create a pattern with intensity distribution described by the following equation

* e-mail: ewa.raczka@ps.pl

$$I(x) = I_0[1 + m \cos(Kx)], \quad (1)$$

where $I_0 = I_1 + I_2$ is the sum of beams intensities,

$$m = 2(I_1 I_2)^{1/2} / I_0, \quad (2)$$

is the modulation depth, $K = 2\pi/\Lambda$ is the grating vector, $\Lambda = \lambda/2\sin\theta$ denotes the space period of the pattern and θ is the interfering beams incidence angle. In bright regions of the interference pattern, the photogeneration of electrons and holes occurs. Free carriers drift to dark regions under the influence of the external electric field and diffusion. There the carriers are trapped. The resulting distribution of space charge is the source of the internal electric field. The space-charge field can be determined by solving the set of material equations based on Kukhtarev-Vinetskii model [15]. For small values of m , the space-charge field can be described by a sine function of the same space period as the interference pattern. For higher values of the modulation index, the electric field is usually presented in the form of a complex Fourier series [16]

$$E(x) \cong E_0 + \sum_{n=1}^N E_n \exp(inKx) + c.c. \quad (3)$$

However, for small intensities of the interfering beams, $I_0 < 1 \text{ W/cm}^2$, and high enough density of traps, $N_D > 10^{17} \text{ cm}^{-3}$, which is typical for most of photorefractive MQW samples, the space-charge electric field intensity can be approximated by [17]

$$E_{sc}(x) = E_0 \frac{\sqrt{1 - m_1^2} - 1 - m_1(\cos(Kx) - \xi \sin(Kx))}{1 + m_1 \cos(Kx)}, \quad (4)$$

where $m_1 = m/(1 + K^2 L_D^2 \xi)$, $\xi = (\mu_e \tau_e - \mu_h \tau_h)/(\mu_e \tau_e + \mu_h \tau_h)$ is so called competition factor between electrons and holes, and

$$L_D^2 = 2 \frac{k_B T}{q} \left(\frac{1}{\mu_h \tau_h} + \frac{1}{\mu_e \tau_e} \right)^{-1}$$

is a bipolar diffusion length. μ_e and μ_h denote the mobilities of electrons and holes, τ_e and τ_h the average lifetimes of electrons and holes, k_B is the Boltzman constant, T is the temperature, and q is the electron charge. In the case of AlGaAs/GaAs MQW structure, the range of E_{sc} described by the model is restricted to few kV/cm because of the transport nonlinearity existing in GaAs [18].

The total electric field causes a refractive index change, which is given approximately by the following equation [19]

$$\Delta n(x) = 1/2 n_0^3 s E(x)^2, \quad (5)$$

where n_0 is the unperturbed refractive index of the considered structure, s denotes a quadratic electrooptic coefficient, and $E(x) = E_0 + E_{sc}$ is the total electric field intensity.

Figure 1 shows the electric field intensity distribution created by the interference pattern with spatial periods 6 μm , 8 μm , and 12 μm . The influence of external electric field E_0 and modulation index m on $E(x)$ are presented. As

one can see, for $m > 0.4$ the electric field distribution considerably differs from the shape of the sine function. The difference increases for higher modulation index values and also for higher external electric field intensities.

The propagation of a monochromatic light beam in the considered structure is described by the following equation

$$\nabla^2 E^{opt} + (k_0 n(x, y, z))^2 E^{opt} = 0, \quad (6)$$

where E^{opt} is the electric field intensity of the wave guided in an array, $k_0 = 2\pi/\lambda$ is a free space wave vector and $n(x, y, z)$ includes the changes of the refractive index due to the interference pattern. The solution of Eq. (6) describing the wave propagating along the optically induced channels can be presented in the form of

$$E^{opt}(x, y, z) = U(x, z)\psi(y)\exp(-in_{ef}k_0 z), \quad (7)$$

where the beam is guided in z direction and x is the transverse coordinate. The planar waveguide layers are perpendicular to y axis, $\psi(y)$ denotes the transverse profile and n_{ef} the effective refractive index of the planar waveguide mode. Evolution of the beam amplitude in the considered structure is described by

$$\frac{\partial U}{\partial z} - \frac{i}{2n_{ef}k_0} \frac{\partial^2 U}{\partial x^2} - ik_0 \Delta n_{ef} U = 0, \quad (8)$$

where

$$\Delta n_{ef} = \frac{1}{2} n_{ef}^3 s E(x)^2 \frac{\int_0^h |\psi(y)|^2 dy}{\int_{-\infty}^{\infty} |\psi(y)|^2 dy}, \quad (9)$$

and h is the MQW layer thickness. Frequency of the guided mode must be chosen in the region of small absorption to allow propagation along the waveguides. On the other hand, small absorption reduces the number of free carriers generated by the guided wave and their influence on the lattice. Equation (8) was solved by finite difference beam propagation method (FD BPM) [20]. The parameters assumed in the calculation are shown in Table 1.

Table 1. Parameters used in calculations.

Writing wavelength	$\lambda = 630 \text{ nm}$
Writing light intensity	$I_0 = 10 \text{ mW/cm}^2$
Fringes contrast	$m = 0-0.8$
Reading wavelength	$\lambda = 845 \text{ nm}$
External electric field	$E_a = 1-4 \text{ kV/cm}$
Electrooptic coefficient	$s = 7 \times 10^{-7} \text{ m}^2/\text{V}^2$
Average refractive index of MQW layer	$n_0 = 3.55$
Effective refractive index	$n_{eff} = 3.548$
Width of computational window	$L_x = 600 \mu\text{m}$
Step simulation in x direction	$\Delta x = 0.2 \mu\text{m}$
Step simulation in z direction	$\Delta z = 1 \mu\text{m}$

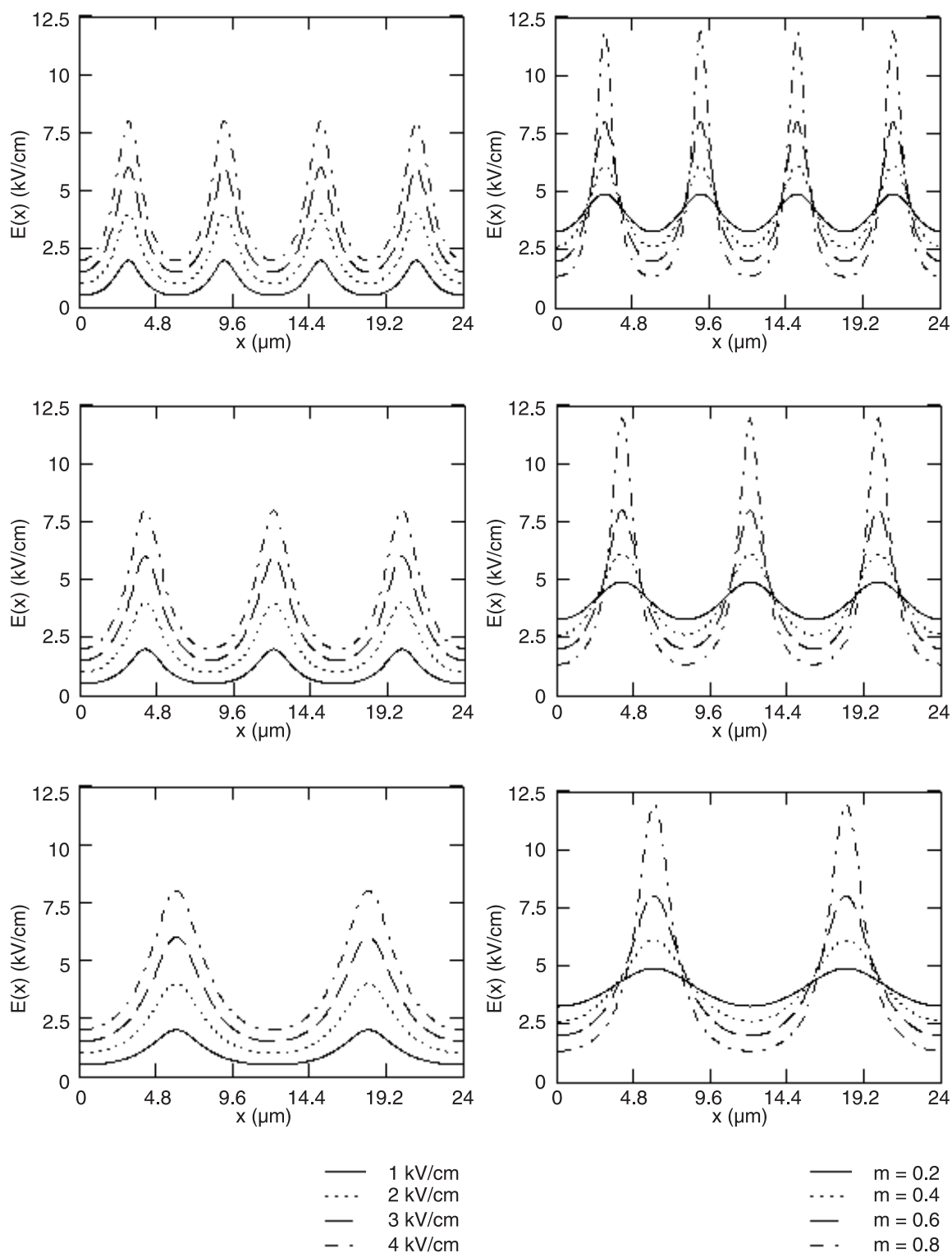


Fig. 1. Electric field distribution induced by the interference pattern with space period $\Lambda = 6 \mu\text{m}$ (a), $\Lambda = 8 \mu\text{m}$ (b), and $\Lambda = 12 \mu\text{m}$ (c) for different external electric field intensities ($E_0 = 1\text{--}4 \text{ kV/cm}$) and modulation depths ($m = 0\text{--}0.8$).

3. Inline propagation

To determine the diffraction properties of the structure we considered influence of the external electric field E_0 and the interference pattern modulation index m on propagation in an array with the space period $\Lambda = 8 \mu\text{m}$. The input light

intensity distribution was described by Gauss function with the peak intensity $I_0 = 0.3 \text{ mW/cm}^2$ and the radius $w_0 = 2.5 \mu\text{m}$, which caused the excitation of only one waveguide in the array. The light intensity value was chosen to make the number of carriers generated by a guided wave much smaller than those generated by the external waves.

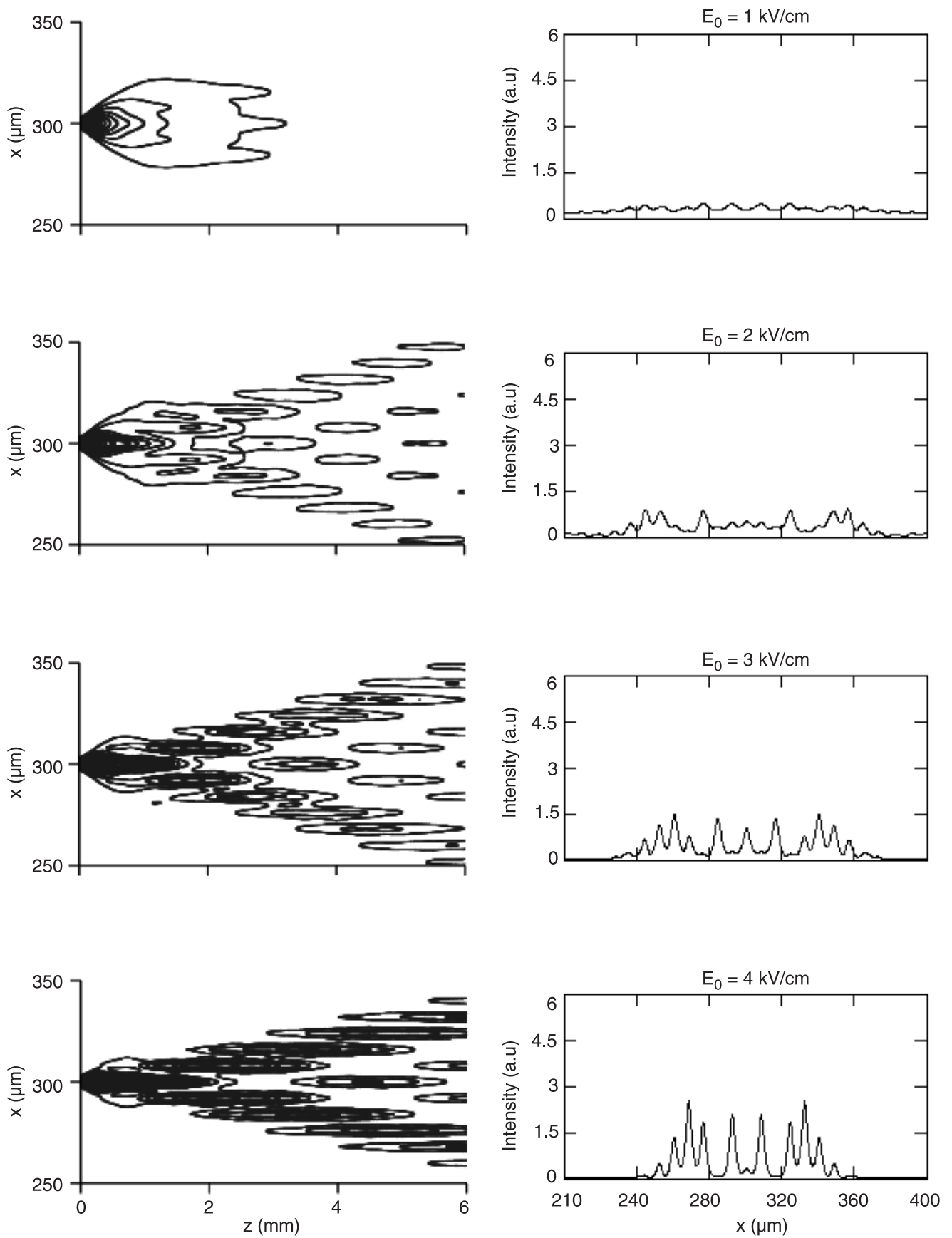


Fig. 2. Propagation in array with space period $\Lambda = 8 \mu\text{m}$ for constant $m = 0.6$ and different external electric field intensities, $E_0 = 1-4 \text{ kV/cm}$.

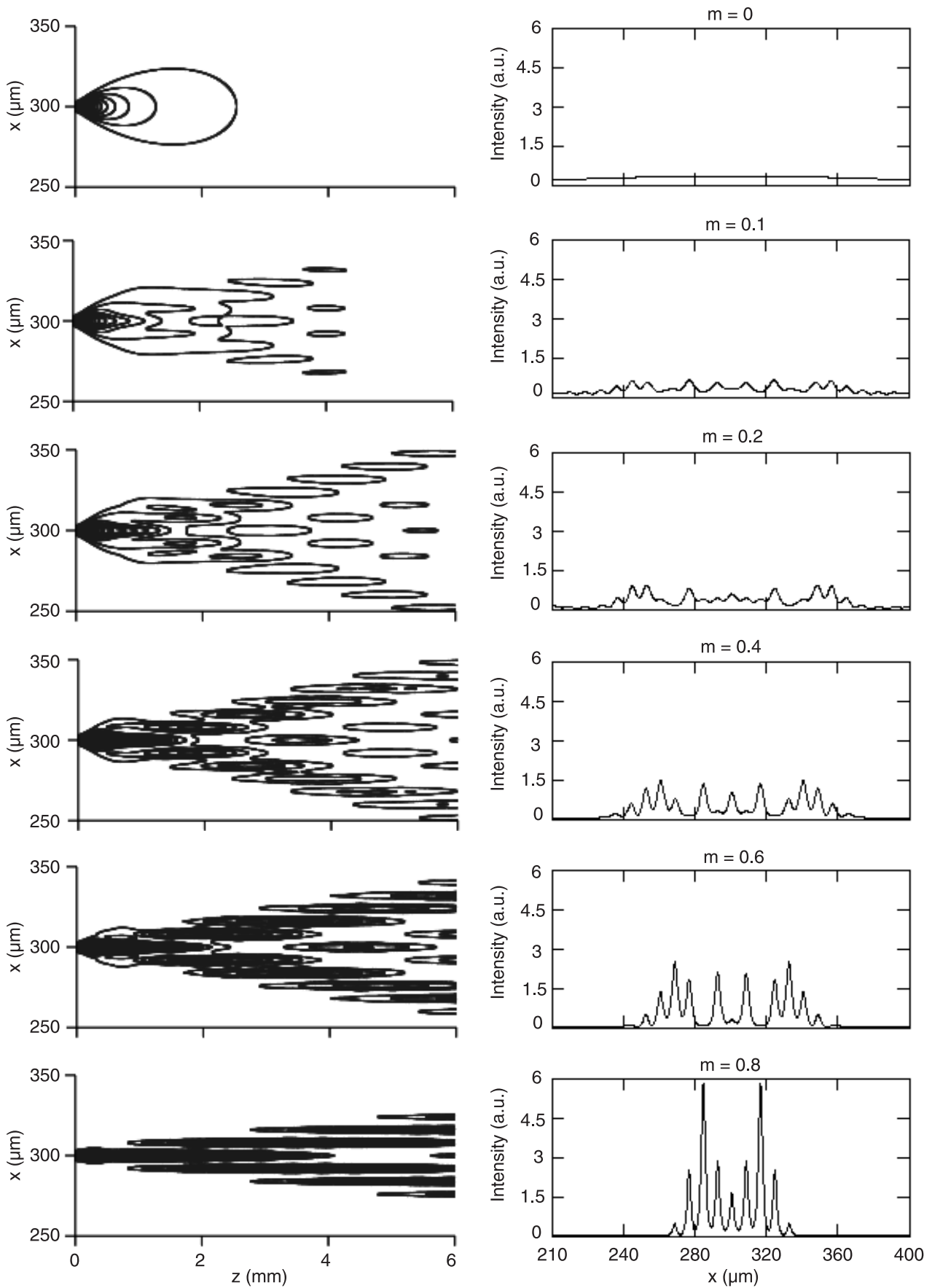


Fig. 3. Propagation in array with the space period $\Lambda = 8 \mu\text{m}$ for the constant $E_0 = 4 \text{ kV/cm}$ and different modulation depths.

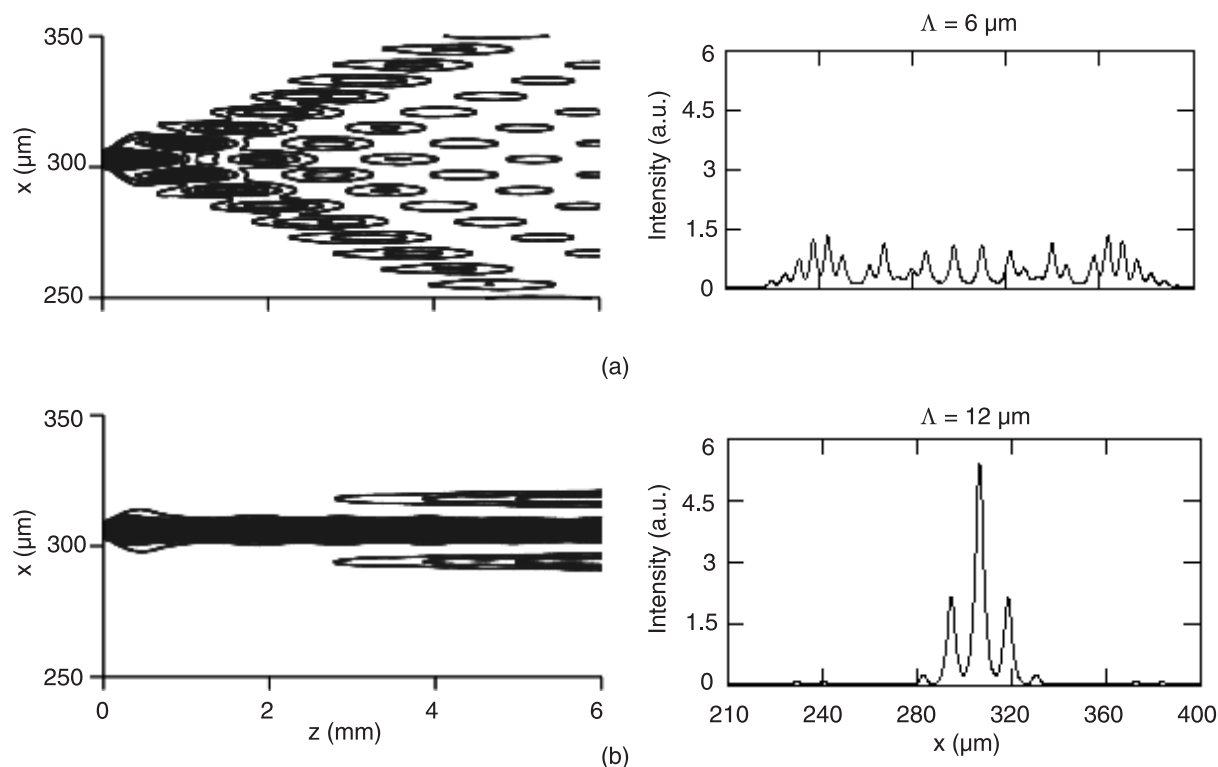


Fig. 4. Propagation in arrays with different space periods $\Lambda = 6 \mu\text{m}$ (a) and $\Lambda = 12 \mu\text{m}$ (b) for $m = 0.6$ and $E_0 = 4 \text{ kV/cm}$.

Figure 2 shows influence of the external electric field intensity on light wave propagation for the constant interference pattern modulation depth, $m = 0.6$. The growth of the external field intensity increases the localization of light in optically induced waveguides and decreases diffraction. To investigate influence of the modulation coefficient m , we took a constant value of the external electric field, $E_0 = 4 \text{ kV/cm}$ and we changed m in the range from 0 to 0.8.

The results presented in Fig. 3 show characteristic discrete diffraction images, with the higher intensity in side lobes than in the central waveguide, for all considered values of m above 0.1. Increasing the value of the modulation index we distinctly observe the decrease in diffraction in the array. Similar influence of E_0 and m changes, shown in the figures, confirm the dependence of the diffraction properties on one parameter which is the coupling coefficient.

To check the influence of the grating period on properties of the lattice we investigated propagation of the narrow beam in the 6- μm and 12- μm lattices. The examples are shown in Fig. 4. In the case of small period, the overlapping of the field from neighbouring channels is so strong that the discrete character of diffraction vanishes. The beam broadening is stronger than in the array with a higher space period for the same values of E_0 and m . On the other hand, increasing of the grating period decreases the coupling between the channels and causes the narrowing of the beam.

The possibility of switching light between outputs of adjacent channels by changing interference pattern modulation depth is shown in Fig. 5.

4. Tilted beam propagation

To confirm the discrete character of the diffraction, we investigated the influence of grating parameters on propagation of a tilted input beam with the diameter w_0 . The incidence angle 0.4° was chosen to obtain transverse component of the wave vector $k_x = \pi/2d$ (where d is the distance between the channels), corresponding to propagation with zero diffraction [1]. The results for the case of lattice period $\Lambda = 8 \mu\text{m}$ and the incidence beam width $w_0 = 15 \mu\text{m}$ are presented in Fig. 6. Increase in the modulation index m causes decrease in the coupling between waveguides which results in stronger influence of “discreteness”. This is the reason of a diffraction decrease or stoppage due to zero diffraction angle, which is shown in Fig. 6(b). Also the direction of propagation changes with increasing m (or E_0).

Trapping of the beam in the input channels is not possible in this array because too high grating amplitudes are required. To show the trapping we considered propagation in the array with space period $\Lambda = 12 \mu\text{m}$. The results for the initial beam width $w_0 = 20 \mu\text{m}$ and the incidence angle 0.3° are shown in Fig. 7. Increase in the space period of the array causes smaller broadening of light intensity distribution in case of rectilinear propagation (see Fig. 4) and increases the constraint of the tilted beam in case of $k_x = \pi/2d$.

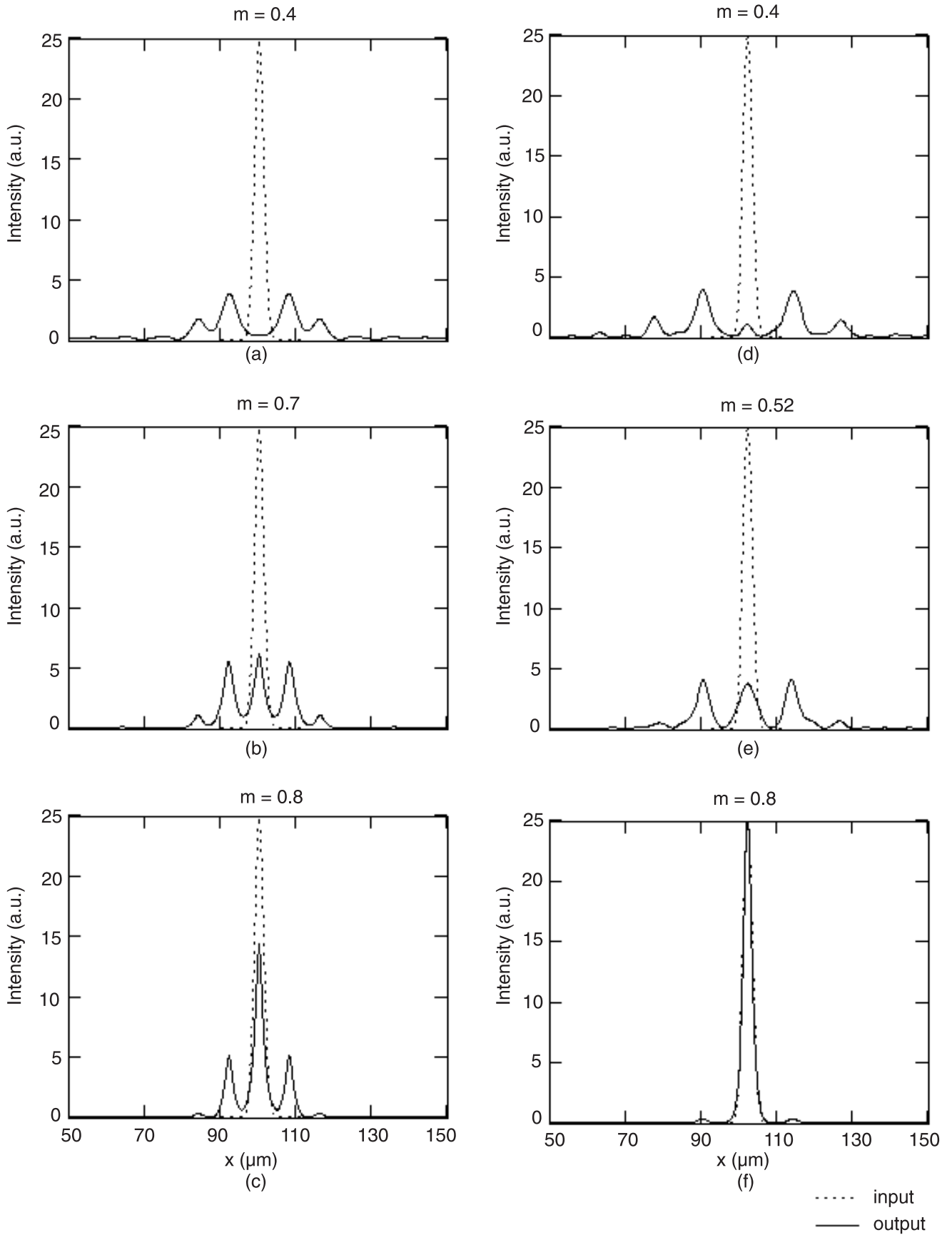


Fig. 5. Output light distribution (a–c) in array with $\Lambda = 8 \mu\text{m}$, propagation distance 2 mm, modulation depth $m = 0.4$, $m = 0.7$, $m = 0.8$ respectively, and (d–f) in array with $\Lambda = 12 \mu\text{m}$, propagation distance 6 mm, $m = 0.4$, $m = 0.52$, and $m = 0.8$.

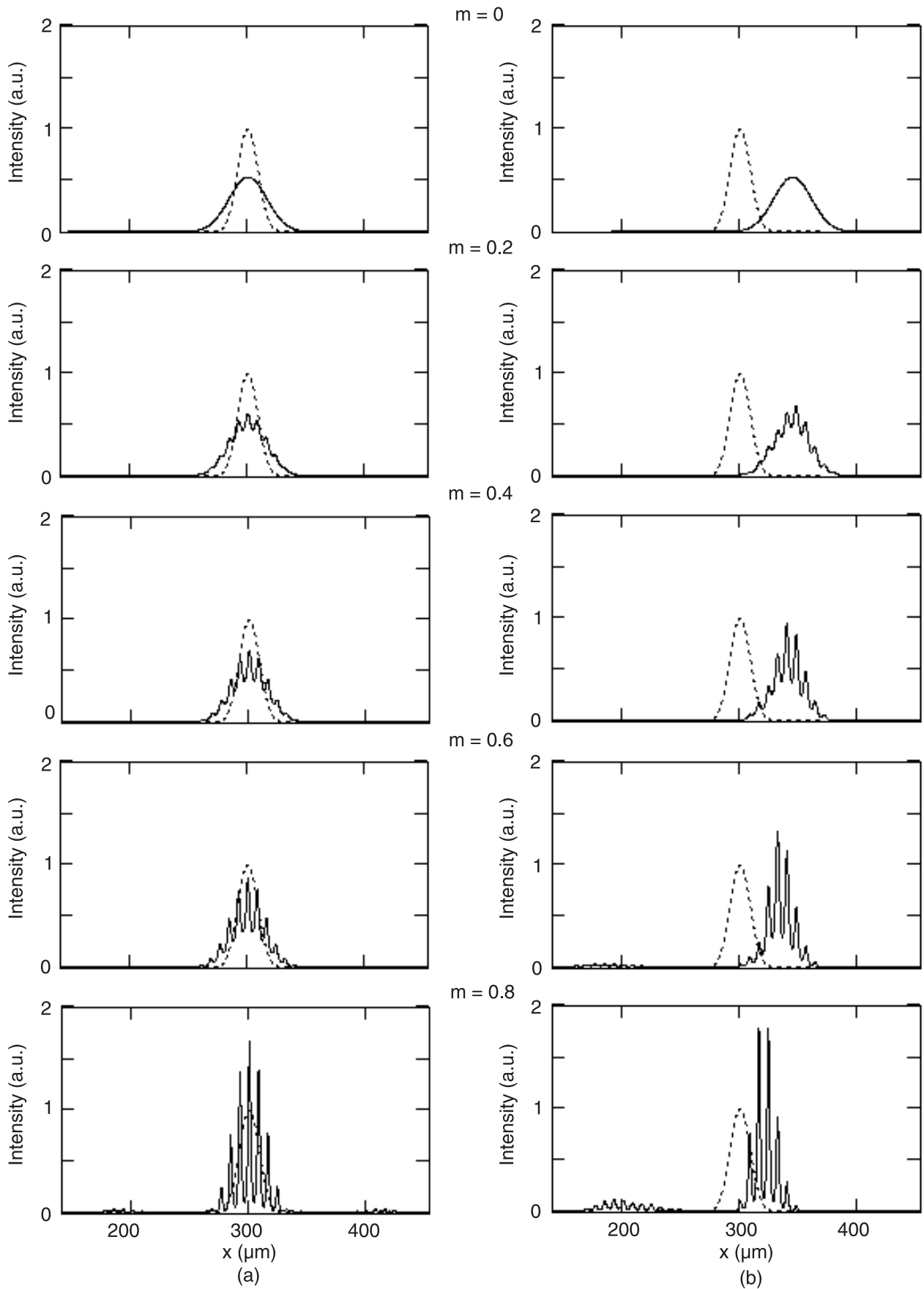


Fig. 6. The influence of modulation depth m on rectilinear ($k_x d = 0$) (a) and tilted ($k_x d = \pi/2$) (b) beam propagation in $\Lambda = 8 \mu\text{m}$ array with constant $E_0 = 4 \text{ kV/cm}$.

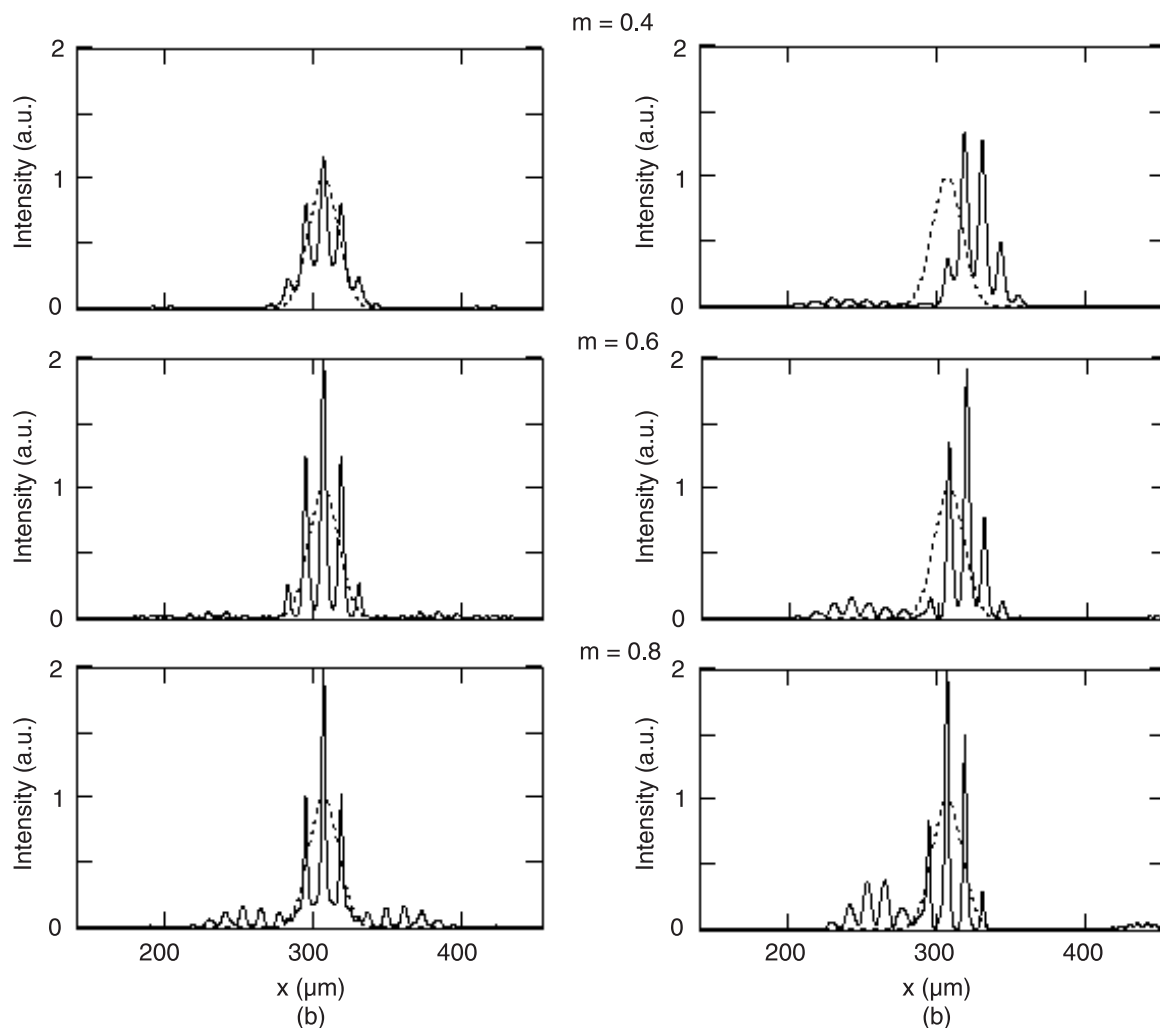


Fig. 7. The influence of modulation depth m on rectilinear ($k_x d = 0$) (a) and tilted ($k_x d = \pi/2$) (b) beam propagation in $\Lambda = 12 \mu\text{m}$ array with the constant $E_0 = 4 \text{ kV/cm}$.

5. Conclusions

The analysis of properties of photorefractive grating generated by two coherent external waves interfering in material with a quadratic relation between the refractive index and electric field intensity confirms the possibility of application of this structure as one dimensional waveguide array. The characteristic discrete diffraction manifested with higher light intensity in two side lobes than in the middle of the beam was found even at small interference pattern modulation depth and moderate intensity of the electric field applied to the sample. It was shown that the degree of system discreteness can be regulated, from common to discrete diffraction, by changing interference pattern modulation depth, electric field intensity or external waves incident angles.

The dependence of coupling between induced channels on the parameters of waves that generate the grating and on the electric field intensity makes the continuous regulation of guided beam width and propagation angle possible.

The calculations presented here were conducted for material parameters characteristic for photorefractive MQW in planar waveguide geometry. The waveguide structure, small light intensity needed to generate the array, the possibility of changing the width and propagation angle of the guided beam by changing the intensity of one of interfering waves suggest the experimental attractiveness of the system. Nonlinear propagation, interactions between waves and generation of discrete solitons are interesting field for further studies.

References

1. D.N. Christodoulides, F. Lederer, and Y. Silberberg, "Discretizing light behaviour in linear and nonlinear waveguide lattices", *Nature* 422, 817 (2003).
2. H.S. Eisenberg, Y. Silberberg, R. Morandotti, and J.S. Aitchison, "Diffraction management", *Phys. Rev. Lett.* 85, 1863 (2000).
3. A.A. Sukhorukov, Y.S. Kivshar, H.S. Eisenberg, and Y. Silberberg, "Spatial optical solitons in waveguide arrays", *IEEE J. Quantum Electron.* 39, 31 (2003).

4. F. Lederer, S. Darmanyan, and A. Kobayakov, "Discrete solitons" in *Spatial Optical Solitons*, Vol. 82, pp. 269–292, edited by S. Trillo and W.E. Torruellas, Springer-Verlag, New York, 2001.
5. N.K. Efremidis, S. Sears, and D.N. Christodoulides, "Discrete solitons in photorefractive optically induced photonic lattices", *Phys. Rev.* **E66**, 046602 (2002).
6. J.W. Fleisher, T. Carmon, and M. Segev, "Observation of discrete solitons in optically induced real time waveguide arrays", *Phys. Rev. Lett.* **90**, 023902 (2003).
7. D. Neshev, E. Ostrovskaya, Y. Kivshar, and W. Królikowski, "Spatial solitons in optically induced gratings", *Opt. Lett.* **28**, 710 (2003).
8. D. Neshev, A.A. Sukhorukov, B. Hanna, W. Królikowski, and Y.S. Kivshar, "Controlled generation and steering of spatial gap solitons", *Phys. Rev. Lett.* **93**, 083905 (2004).
9. A.A. Sukhorukov, D. Neshev, W. Królikowski, and Y.S. Kivshar, "Nonlinear Bloch-wave interaction and Bragg scattering in optically induced lattices", *Phys. Rev. Lett.* **92**, 093901 (2004).
10. Y.V. Kartashov, V.A. Vysloukh, and L. Torner, "Tunable soliton self-bending in optical with nonlocal nonlinearity", *Phys. Rev. Lett.* **93**, 153903 (2004).
11. A.S. Desyatnikov, E. Ostrovskaya, Y.S. Kivshar, and C. Denz, "Composite band-gap solitons in nonlinear optically induced lattices", *Phys. Rev. Lett.* **91**, 153902 (2003).
12. D. Neshev, Y.S. Kivshar, H. Martin, and Z. Chen, "Soliton stripes in two-dimensional nonlinear photonic lattices", *Opt. Lett.* **29**, 486 (2004).
13. Z. Chen, H. Martin, E.D. Eugenieva, J. Xu, and A. Bezryadina, "Anisotropic enhancement of discrete diffraction and formation of two-dimensional discrete-soliton trains", *Phys. Rev. Lett.* **92**, 143902 (2004).
14. E. Weinert-Rączka, M. Wichtowski, A. Ziótkowski, and G. Staroń, "Photorefractive grating in multiple quantum well planar waveguide", *Acta Physica Polonica* **A103**, 229 (2003).
15. N.V. Kukhtarev, V. Markov, S. Odulov, M. Soskin, and V. Vinetskii, "Holographic storage in electrooptic crystal. 1 Steady state", *Ferroelectrics* **22**, 949 (1979).
16. Q. Wang, R.M. Brubaker, D.D. Nolte, and M.R. Melloch, "Photorefractive quantum wells: transverse Franz-Keldysh geometry", *J. Opt. Soc. Am.* **B9**, 1626 (1992).
17. M. Wichtowski, E. Weinert-Rączka, and A. Gajda, "Steady state photorefractive gratings in multiple quantum wells at high modulation depth", **13**, 157–169 (2005) to *Opto-Electron. Rev.*
18. R.M. Brubaker, Q.N. Wang, D.D. Nolte, and M.R. Melloch, "Nonlocal photorefractive screening from hot electron velocity saturation in semiconductors", *Phys. Rev. Lett.* **77**, 4249 (1996).
19. Q.N. Wang, D.D. Nolte, and M.R. Melloch, "Spatial-harmonic gratings at high modulation depths in photorefractive quantum wells", *Opt. Lett.* **16**, 1944–1946 (1991).
20. R. Scarmozzino, and R.M. Osgood Jr., "Finite difference and Fourier-transform solutions of the parabolic wave equation with emphasis on integrated-optics applications", *J. Opt. Soc. Am.* **B8**, 724 (1991).